AFRPL-TR-82-006

UDR-TR-81-158

NONLINEAR COMBUSTION INSTABILITY IN SOLID ROCKET MOTORS:
A NUMERICAL STUDY OF LONGITUDINAL OSCILLATIONS WITH PRESSURE
AND VELOCITY COUPLING
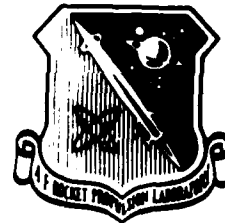
Authors: J. D. Baum   J. N. Levine

University of Dayton   Air Force Rocket Propulsion
Research Institute   Laboratory
Dayton OH 45469   Edwards AFB CA 93523

April 1982

Interim Report for the period February through December 1981

DTIC
SELECTED
JUN 3 1982

D

82 06 01 076

NOTICE

This technical report is approved for release and distribution in accordance with the distribution statement on the cover and on the DD Form 1473.

WILBUR C. ANDREPONT
Task Manager, Combustion
and Plumes

FOR THE DIRECTOR

JAMES T. EDWARDS
Chief, Plans and Programs

REPORT DOCUMENTATION PAGE	READ INSTRUCTIONS BEFORE COMPLETING FORM

1. REPORT NUMBER	2. GOVT ACCESSION NO.	3. RECIPIENT'S CATALOG NUMBER
AFRPL-TR-82-006	AD-A115084	

4. TITLE (and Subtitle)	5. TYPE OF REPORT & PERIOD COVERED
NONLINEAR COMBUSTION INSTABILITY IN SOLID ROCKET MOTORS: A NUMERICAL STUDY OF LONGITUDINAL OSCILLATIONS WITH PRESSURE AND VELOCITY COUPLING	Final February 1981-December 1981
	6. PERFORMING ORG. REPORT NUMBER UDR-TR-81-158

7. AUTHOR(s)	8. CONTRACT OR GRANT NUMBER(s)
Joseph D. Baum, U Dayton Jay N. Levine, AFRPL	F04611-81-C-0012

9. PERFORMING ORGANIZATION NAME AND ADDRESS	10. PROGRAM ELEMENT, PROJECT, TASK AREA & WORK UNIT NUMBERS
University of Dayton Research Institute Dayton, OH 45469	2308M1UJ

11. CONTROLLING OFFICE NAME AND ADDRESS	12. REPORT DATE
Air Force Rocket Propulsion Laboratory/XRX Edwards Air Force Base, CA 93523	April 1982
	13. NUMBER OF PAGES 41

14. MONITORING AGENCY NAME & ADDRESS(If different from Controlling Office)	15. SECURITY CLASS. (of this report)
	Unclassified
	15a. DECLASSIFICATION/DOWNGRADING SCHEDULE

16. DISTRIBUTION STATEMENT (of this Report)

Approved for public release; Distribution unlimited.

17. DISTRIBUTION STATEMENT (of the abstract entered in Block 20, if different from Report)

18. SUPPLEMENTARY NOTES

19. KEY WORDS (Continue on reverse side if necessary and identify by block number)

Solid Rocket Motors	Two-Phase Flow
Combustion Instability	Velocity Coupling
Nonlinear Instability	
Numerical Analysis	

20. ABSTRACT (Continue on reverse side if necessary and identify by block number)

 An existing nonlinear instability model has been extended and improved to allow it to more realistically treat the longitudinal shock wave type of combustion instability frequently encountered in tactical solid rocket motors. Results obtained utilizing this model to investigate limiting amplitude and velocity coupling phenomena in solid rocket motors are presented. An advanced finite difference integration technique capable of accurately describing shocks and contact discontinuities has been incorporated into the computer program, as well as an improved heat conduction solution, an heuristic velocity coupling

DD FORM 1473 EDITION OF 1 NOV 65 IS OBSOLETE

model, and a spectral analysis capability. Solutions of wave propagation and shock formation and propagation in a variable area duct and a solid propellant rocket motor are presented; as are a number of solutions demonstrating that limiting amplitude is independent of the characteristics of the initial disturbance. Results of a preliminary study of nonlinear velocity modulated limit cycles are presented, as are results that demonstrate the primarily traveling wave nature of nonlinear wave propagation in solid rocket motors, and the complexity of the phase relationships between pressure, burning rate, and velocity oscillations are presented. Finally, the effect of a threshold velocity on nonlinear velocity coupled instability was explored, and some of the results are also presented.

TABLE OF CONTENTS

LIST OF ILLUSTRATIONS

SECTION 1
INTRODUCTION

Nonlinear axial-mode instability in solid propellant rocket motors is initiated by random finite amplitude events such as the expulsion of an igniter or insulation fragment through the nozzle. When an instability is so initiated in a motor otherwise linearly stable (i. e., stable to infinitesimal disturbances) it is said to be a "triggered" instability. The existence of triggered instabilities is a direct result of the fact that all the acoustic energy gain or loss mechanisms in a solid rocket motor, e. g., pressure and velocity-coupled driving, nozzle and particle damping, acoustic mean flow interactions, etc., are nonlinear, i. e., amplitude-dependent to some degree. These same nonlinearities also ensure that a nonlinear instability will not grow without limit but will eventually reach a limit cycle amplitude at which the net gains and losses are balanced.

Nonlinear axial-mode instabilities usually result in pressure oscillations that propagate as steep-fronted waves which are actually weak shock waves. The acoustic pressure and velocity oscillations are frequently accompanied by an increase in mean chamber pressure (usually referred to as a dc shift) and increased mean propellant burn rate. This increased burn rate is thought to be primarily a response to acoustic velocity oscillations. Thus, it is often referred to as acoustic erosivity.

Certain trends and characteristics of nonlinear instability have been documented. However, attempts to form generally applicable conclusions have been stymied by the number, the complexity, and the mutual interactions of the governing physical phenomena. The ability to predict, avoid, or eliminate nonlinear instability is, therefore, clearly contingent upon our ability to understand and model these phenomena.

4

Efforts to understand and model nonlinear instability date back to the 1960's, e. g., References 1 to 3. The most recent work has been divided between so-called "exact" and "approximate" mathematical approaches. The "exact" methods of Levine and Culick[4] and Kooker and Zinn[5] seek to solve numerically the nonlinear partial differential equations governing the mean and time-dependent flow in the combustion chamber, as well as the combustion response of the solid propellant. The "approximate" methods of Culick[6] and Powell, et al.,[7] use expansion techniques to reduce the problem to the solution of sets of ordinary differential equations. Culick and Levine[8] carried out a brief comparison of results with these two approaches and found that within certain limits the approximate techniques yield quite reasonable results. Each of these methods has certain advantages, disadvantages, and limitations regarding accuracy, computation time, generality, etc.

The previously developed "exact" nonlinear instability programs are not capable of treating the multiple travelling shock-wave type of instability

1. Price, E. W., "Axial Mode Intermediate Frequency Combustion Instability in Solid Propellant Rocket Motors," AIAA Preprint No. 64-146 (Jan. 1964).

2. Brownlee, W. G., "Nonlinear Axial Combustion Instability in Solid Propellant Motors," AIAA J. Vol. 2, No. 2 (Feb. 1964) pp. 205-284.

3. Marxman, G. A. and Wooldrige, C. E., "Finite-Amplitude Axial Instability in Solid-Rocket Combustion," Twelfth Symposium (International) on Combustion (The Combustion Institute, Pittsburg, Pa., 1969) pp. 115-127.

4. Levine, J. N. and Culick, F. E. C., "Nonlinear Analysis of Solid Rocket Combustion Instability," AFRPL Technical Report TR-74-45, Oct. 1974.

5. Kooker, D. E. and Zinn, B. T., "Numerical Investigation of Nonlinear Axial Instabilities in Solid Rocket Motors," BRL CR 141, March 1974.

6. Culick, F. E. C., "Nonlinear Behavior of Acoustic Waves in Combustion Chambers," 10th JANNAF Combustion Meeting, Vol. 1, CPIA Publication 243, 1973, pp. 417-436, or California Institute of Technology Report, 1975.

7. Powell, E. A., Padmanabhan, M. S., Zinn, B. T., "Approximate Nonlinear Analysis of Solid Rocket Motors and T-Burners," AFRPL-TR-77-48, 1977.

8. Culick, F. E. C. and Levine, J. N., "Comparison of Approximate and Numerical Analyses of Nonlinear Combustion Instability," AIAA, 12th Aerospace Sciences Meeting, Preprint 74-201, 1974.

that occurs in the reduced minimum smoke tactical motors since developed. Nor do these analyses contain a model for velocity coupling, something which appears to be required to predict the types of triggering events and dc pressure shifts that have been observed. The objective of the present research is to extend and improve the model developed in Reference 4 to the point where it can be used as a tool to enhance our understanding of nonlinear instability, as an aid in the design and interpretation of related experimental work, as a means to evaluate the validity of advanced combustion response models, and as a design aid to solve or prevent nonlinear instability problems.

To reach the stated objective, the numerical techniques used in Reference 4 had to be replaced by a more advanced method, and a model for addressing velocity-coupled effects had to be incorporated into the computer program. Other improvements, such as the ability to analyze the computed wave forms spectrally have also been accomplished.

The ability of finite difference integration methods to solve accurately the one-dimensional, nonlinear, two-phase, hyperbolic equations which govern the propagation of shock waves in combustion chambers was critically investigated.[9] The results showed that excellent results are obtained by employing a combination operator consisting of the Lax-Wendroff scheme[10] hybridized with Harten and Zwas' first order scheme[11] and further modified by an Artificial Compression correction.[12]

---

9. Baum, J. D. and Levine, J. N., "Evaluation of Finite Difference Schemes for Solving Nonlinear Wave Propagation Problems in Rocket Combustion Chambers," AIAA Paper No. 81-0420, presented at AIAA 19th Aerospace Sciences Meeting, St. Louis, MO, Jan. 1981.

10. Lax, P. D. and Wendroff, B., "System of Conservation Laws," Comm. Pure Appl. Math, Vol. 13, 1960, pp. 217-237.

11. Harten, A. and Zwas, G., "Self Adjusting Hybrid Schemes for Shock Computations," J. of Comp. Physics, Vol. 9, 1972, pp. 568-583.

12. Harten, A., "The Artificial Compression Method for Computation of Shock and Contact Discontinuities: III, Self Adjusting Hybrid Schemes," AFOSR Technical Report TR-77-0659, March 1977.

A survey of past attempts to model or predict the effects of velocity coupling on the stability of solid rocket motors leads to the conclusion that very little is now known about velocity coupling. This conclusion is supported by the results of a recent JANNAF workshop on velocity coupling.[13] All existing models appear to have significant deficiencies. Price's original velocity-coupling model[14] is purely empirical. Other investigators sought to modify existing combustion models by introducing an additional source of heat transfer to the propellant surface. For example, in References 15 and 4 a heat transfer term based on an empirical function of velocity was used, while in References 16 to 18, additional heat transfer was included on the basis of modifications to steady-state turbulent boundary-layer theories and/or erosive burning-rate models. All of these models ignore some of the fundamental physics of the problem. Turbulent boundary layers in the usual sense are not typically realized in solid rocket motor chambers.[19] While some of the existing velocity-coupling models properly reduce to steady-state erosive

13. Beckstead, M. W., "Report of the Workshop on Velocity Coupling," presented at 17th JANNAF Combustion Meeting, CPIA Report No. 324, Nov. 1980.

14. Price, E. W. and Dehority, G. L., "Velocity Coupled Axial Mode Combustion Instability in Solid Propellant Rocket Motors," Proceedings of the 2nd ICRPG/AIAA Solid Propulsion Meeting, Anaheim, California (1967) pp. 213-227.

15. Culick, F. E. C., "Stability of Longitudinal Oscillations with Pressure and Velocity Coupling in a Solid Propellant Rocket," Combustion Science and Technology, Vol. 2, No. 4 (1970), pp. 179-201.

16. Lengelle', G., "A Model Describing the Velocity Response of Composite Propellants," AIAA J. Vol. 13, 1975, pp. 315-322.

17. Condon, J. A., "A Model for the Velocity Coupling Response of Composite Propellant," 16th JANNAF Combustion Meeting, Monterey, CA September 1979, CPIA Pub. No. 308, Dec. 1979.

18. Srivastava, R., "Investigation of Chemically Reacting Boundary Layers in Solid Propellant Rockets: Steady and Periodic Solutions," Ph. D. Thesis, Georgia Institute of Technology, 1977.

19. Beddini, R. A., "Effects of Grain Port Flow on Solid Propellant Erosive Burning," AIAA Paper 78-977, 1978.

burning models as the limit of zero frequency is approached, none of them properly treats acoustic boundary-layer effects that become significant in the normal longitudinal frequency range ($\sim$ 200 to 1,000 Hz).[20] In addition, acoustic boundary-layer transition and acoustic turbulence interactions may also be important under certain conditions,[21] as may the interaction of an unsteady boundary layer with the propellant surface structure.

The importance of velocity coupling underlines the need for increased understanding of it. Experimental and analytical investigations have recently been initiated by several researchers. To help guide in the design and interpretation of velocity-coupling experiments and to help validate new velocity-coupled combustion response models, there exists a need for a comprehensive, nonlinear combustion instability model. The authors have been developing such a model[4,9] and have recently extended it to include the ability to treat nonlinear velocity-coupling effects.[22]

Due to the aforementioned deficiencies of currently existing models, no velocity-coupling model was selected for incorporation into the nonlinear stability program. Instead, calculations were performed using several different ad hoc functions of velocity to augment directly either the heat transfer to the propellant surface or the transient burning rate itself. The solutions[22] demonstrated many of the nonlinear characteristics observed in actual solid rocket motor firings, e. g., steep-fronted waves, triggering, formation of limit cycles, including those with modulated amplitudes, and increases in mean operating pressure (dc shift). The results also demonstrated the inability of velocity-coupling models based on standard quasi-steady gas phase, homogeneous solid phase assumptions to generate strong nonlinear effects.

---

20. Flandro, G. A., "Solid Propellant Acoustic Admittance Correlations," J. of Sound and Vibration, 36, 1974, pp. 297-312.

21. Beddini, R. A., to be published.

22. Levine, J. N. and Baum, J. D. "A Numerical Study of Nonlinear Instability Phenomena in Solid Rocket Motors," AIAA/SAE/ASMA 17th Joint Propulsion Conference, July 27-29, 1981, Colorado Springs, Colorado, Paper Number AIAA-81-1524.

This report presents some of the most significant results with the improved model, including: (a) a demonstration of the ability of the developed model to treat multiple shock-wave propagation in variable cross-sectional area ducts and solid propellant rocket motors and (b) the effect of initial disturbance amplitude and wave form, combustion response, and particle concentration upon limiting amplitude. This report also presents results that demonstrate the complexity and importance of the phase relationships between pressure, burning rate, and velocity oscillations in the presence of traveling waves and results which briefly examine threshold velocity effects on non-linear velocity-coupled instability.

SECTION 2
VARIABLE AREA DUCTS AND COMBUSTION CHAMBERS

Most practical tactical rocket motor grain configurations have a variable cross-sectional port area. When the rate at which the area varies becomes relatively rapid, or in the limit, discontinuous, the propagating shock wave type of instability previously discussed becomes even more complex. If a shock wave is traveling from a large area section to a smaller one, part of the shock wave is transmitted and part is reflected. Thus, two shock waves, and correspondingly two contact discontinuities, are created. In the opposite situation, when a shock travels from a small area to a larger one, the shock wave is transmitted and an expansion fan is reflected. In an actual motor both of these processes occur repeatedly, creating a very complicated wave structure in the chamber. The presence of such multiple shock-wave systems in variable cross-sectional motors has been confirmed experimentally.[23]

The problem of calculating shock wave propagation phenomena in variable area chambers is clearly a severe test of a finite difference scheme's ability to capture several shocks and describe them in a sharp nonoscillatory manner, even after many wave cycles. To evaluate the ability of Lax Wendroff + Hybrid + Artificial Compression technique to treat such complex problems, a simple closed-duct problem was solved initially.

The geometry considered is shown in Figure 1. The solution was initiated with a continuous disturbance having an amplitude equal to 20% of the mean chamber pressure (1,000 psi) and a wave form given by $\cos(\pi X/L)$ (all of the initial disturbances for solutions presented in this report used this wave form, and the percentage given is the zero to peak amplitude of the oscillatory wave form as a percentage of the mean pressure). The solution was continued for approximately 30 complete wave cycles (nondimensional time equal 60). The initially smooth sine wave quickly steepens into a traveling

---

23. Hughes, P. M., and Smith D. L., "Nonlinear Combustion Instability In Solid Propellant Rocket Motors. Influence of Geometry and Propellant Formulation," 53rd AGARD Meeting, Propulsion and Energetics Panel, Oslo, Norway, April, 1979.
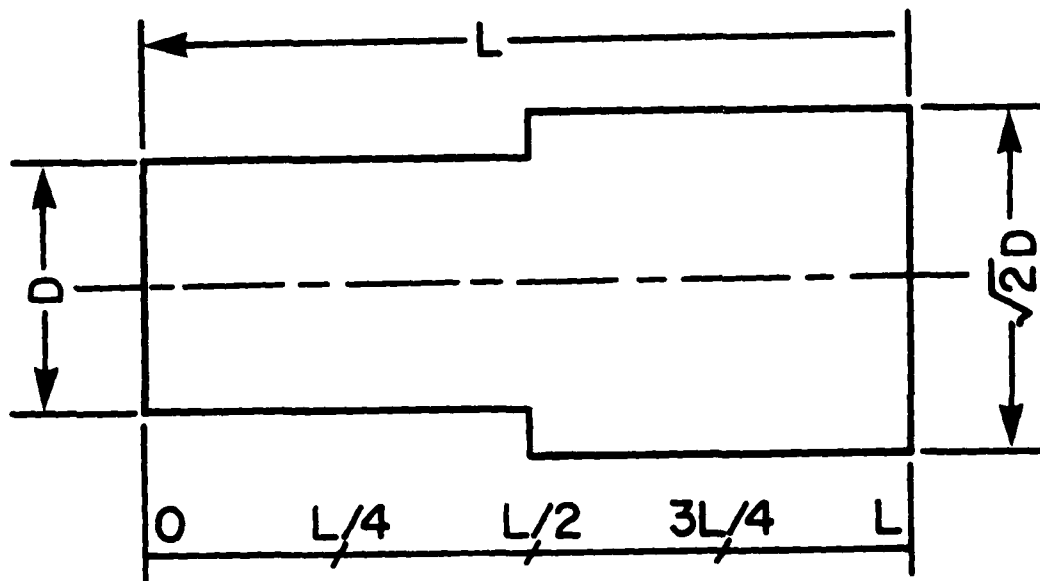
Figure 1. Variable Area Duct Geometry.

shock wave which, as previously discussed, is then repeatedly reflected and transmitted as it encounters the area discontinuity and ends of the tube.

Figure 2 shows the calculated wave forms and respective power spectral densities at five different locations along the tube for the ninth and tenth wave cycles. As expected, the wave forms are quite complex, and both the wave forms and their spectra vary significantly from one location to another. Based on comparisons with experimental results from cold-gas pulse tests, the analytical solution appears to portray accurately the physics of this complex problem.[24]

The wave form at the left end of this test problem is dominated by a single shock wave and a single expansion fan. One should notice the sharp,

----

24. Lovine, R., Aerojet Tactical System, Private Communication.

11
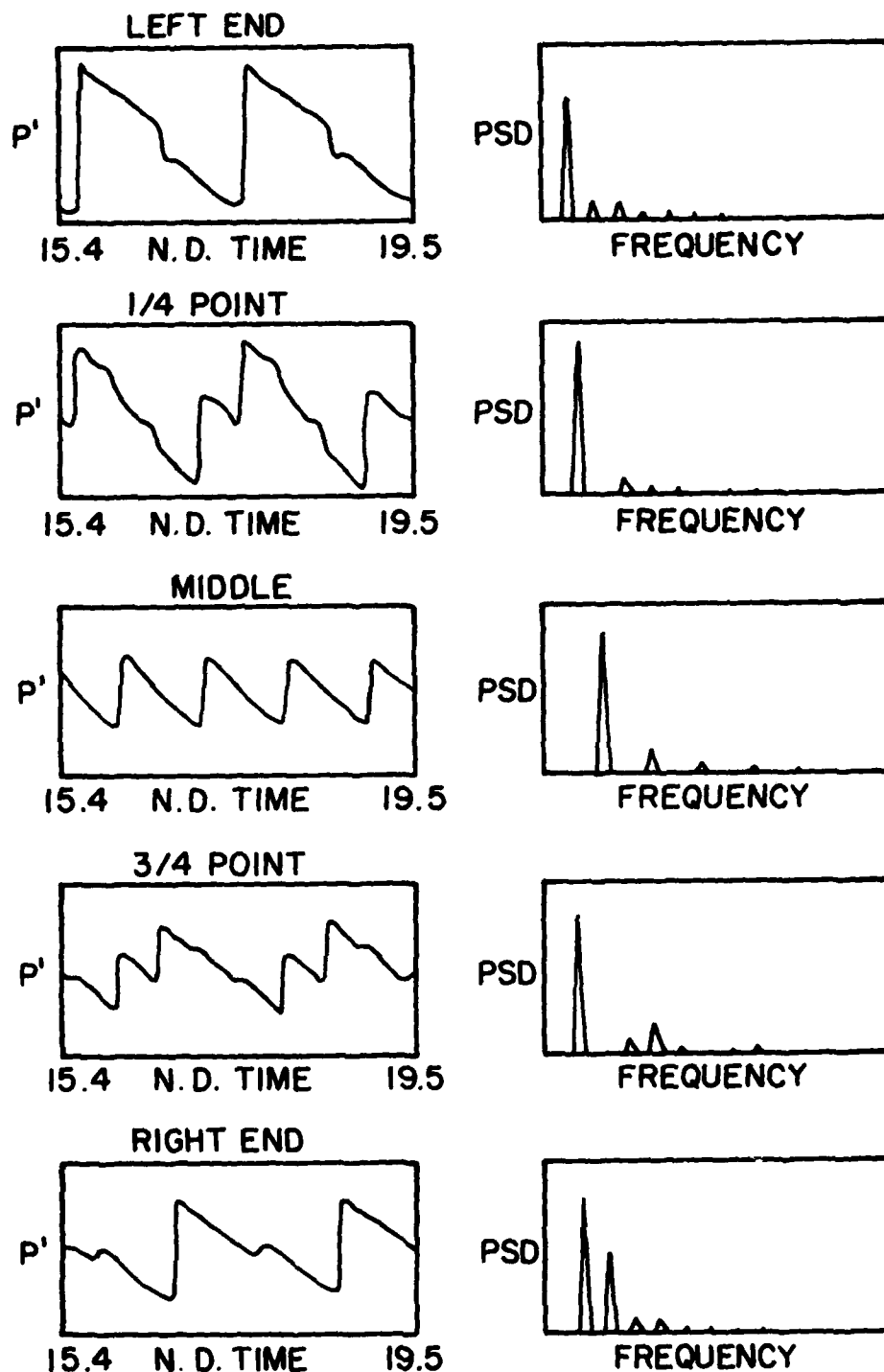
Figure 2. Expanded Views of the Calculated Pressure Histories and Power Spectral Densities at Five Locations Along a Duct with an Area Jump, $\Delta p_0' = 0.2 \cos (\pi X/L)$.

nonoscillatory captured shock, even after many reflections. At the ¼ point, two relatively strong shock waves, two weak shocks, and two expansions are in evidence. The spectral analysis indicates that the second and sixth harmonics are missing, as should be expected. The wave form in the middle consists of traveling shock waves at a frequency double that of the ends, with half the amplitude. The main features at the 3/4 and right-end points are four and two shock waves, respectively. One should notice the strong, augmented, even harmonics at these locations. Since most of the significant acoustic gain and loss mechanisms in solid rocket motors are quite frequency-dependent, the strong axial variations in harmonic content in chambers with sharply varying cross-sectional areas can be expected to have a significant effect upon motor stability, an effect completely unpredictable on the basis of linear stability analysis.

Following the successful solution of the test problem, a solid rocket motor problem having the same geometry as Figure 1 (but with a nozzle at the right end) was solved to demonstrate the capability of the developed model to solve such problems in the presence of mean flow and combustion. Figure 3 shows the calculated pressure wave forms at the left end and ¼ points of the

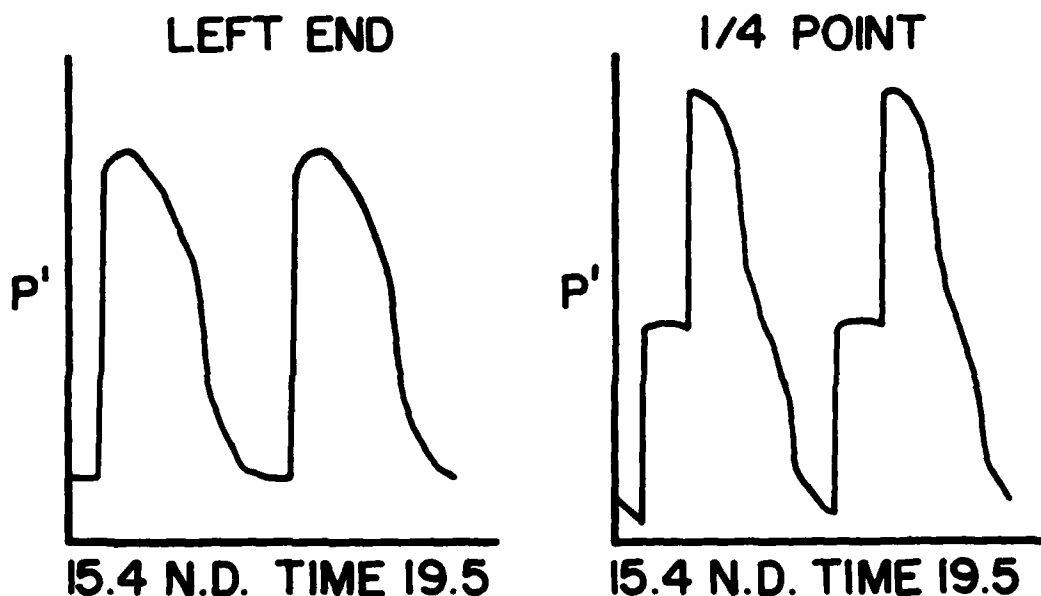Figure 3. Expanded View of the Calculated Pressure History at Two Locations Along the Motor with an Area Jump, $\Delta p'_0 = 0.2 \cos (\pi X/L)$.

13

motor. Except for the rounded tops (attributable to different distribution of
energy among the respective harmonics caused by mean flow and complex nozzle
end admittance) the waveforms are quite similar to those obtained in the
closed duct problem.

SECTION 3
LIMITING AMPLITUDE STUDIES

From a practical standpoint, the ability to predict the limiting ampli-
tude reached by pressure oscillations in unstable solid rocket motors is
important in assessing whether such an instability will be severe enough to
warrant design or propellant modifications to eliminate it. For both prac-
tical and theoretical reasons, it is also important to establish whether limit
cycles are unique, i. e., independent of the characteristics of the initiating
disturbance.

Even under the most carefully controlled laboratory conditions, it is
almost impossible to conduct a series of motor firings in which the only
variable is either initial disturbance amplitude or waveform. To the authors'
knowledge, no test series has ever been conducted for the primary purpose of
establishing the effect of initial disturbance on limiting amplitude. Results
from some tests which approximate the required conditions are not definitive.
However, on balance they favor a conclusion that limiting amplitude is inde-
pendent of the initiating disturbance. It should be emphasized that the above
refers to the limit amplitude reached if a motor is pulsed into instability.
It has been clearly demonstrated that the triggering event itself is dependent
on pulse characteristics.

The difficulty in experimentally examining the uniqueness of limit cycles
makes the analytical examination of this question all the more important. The
question has been previously addressed for liquid[25, 26] and solid[4, 6, 7, 9]
rocket motors using expansion and numerical techniques. Results from expan-
sion solutions indicate that the limit cycle should be independent of the ini-
tiating disturbance. However, since these methods have limits in regard to
their applicability to strongly nonlinear situations with very high amplitudes

25. Zinn, B. T. and Powell, E. A., "Nonlinear Combustion Instability in
Liquid Propellant Rocket Engines," Proceedings of the 13th Symposium
(International) on Combustion, The Combustion Institute, 1971, pp.
491-503.

26. Powell, E. A. and Zinn, B. T., "The Prediction of Nonlinear
Three-Dimensional Combustion Instability in Liquid Rockets with
Conventional Nozzles," NASA CR-121279, October 1973.

and/or shock-like wave forms, and since not all of the nonlinearities present in tactical solid rocket motors were incorporated in the models, the conclusion must be regarded as relevant but requiring further substantiation.

Previous results with the present "exact" model seemed to yield apparently conflicting conclusions. Results obtained in Reference 4, for motors with a particle-to-gas-weight flow ratio of 0.36 and 2-micron particles appeared to demonstrate that limiting amplitude is a strong function of initial disturbance amplitude. Conversely, solutions obtained for almost identical conditions without particles[9] yielded the same limiting amplitude for both standing-wave and pulse-type initial disturbances of widely varying amplitude. It was tentatively concluded that the apparently conflicting results were due to nonlinear particle damping effects. Since this previous conclusion was based on a limited number of results, it was decided to obtain several more sets of solutions, with and without particles.

The series of results shown in Figure 4 are for a cylindrically perforated motor 59.7 cm (23.5 in) long with a port area of 21.5 cm^2 (3.33 in^2), a throat area of 2.83 cm^2 (.439 in^2), and a chamber pressure of 13.19 MPa (1913 psi). These calculations were performed for a propellant without particles and with a linear pressure-coupled response function of 5.35 (no velocity coupling). The solutions were initiated by perturbing the steady state with fundamental mode disturbances of varying amplitude. The calculated pressure perturbation histories at the head end of the motor are shown for initial amplitudes of 40%, 8%, and 2% of the mean pressure. Other solutions were also obtained for amplitudes of 60% and 10% of the mean pressure. All the solutions reached the same limiting amplitude, 32.7% of the mean pressure (peak to peak).

Additional solutions for the same motor and operating conditions were obtained with several other pressure-coupled response functions. All the solutions for a given response function reached the same limiting amplitude, but each response function produced a somewhat different limiting amplitude.

Several other series of calculations were then performed with varying sizes and amounts of particles to reexamine the conclusion reached in Reference 4. The first series of calculations (with the same motor geometry used in the results shown in Figure 4) were conducted with 2-micron aluminum
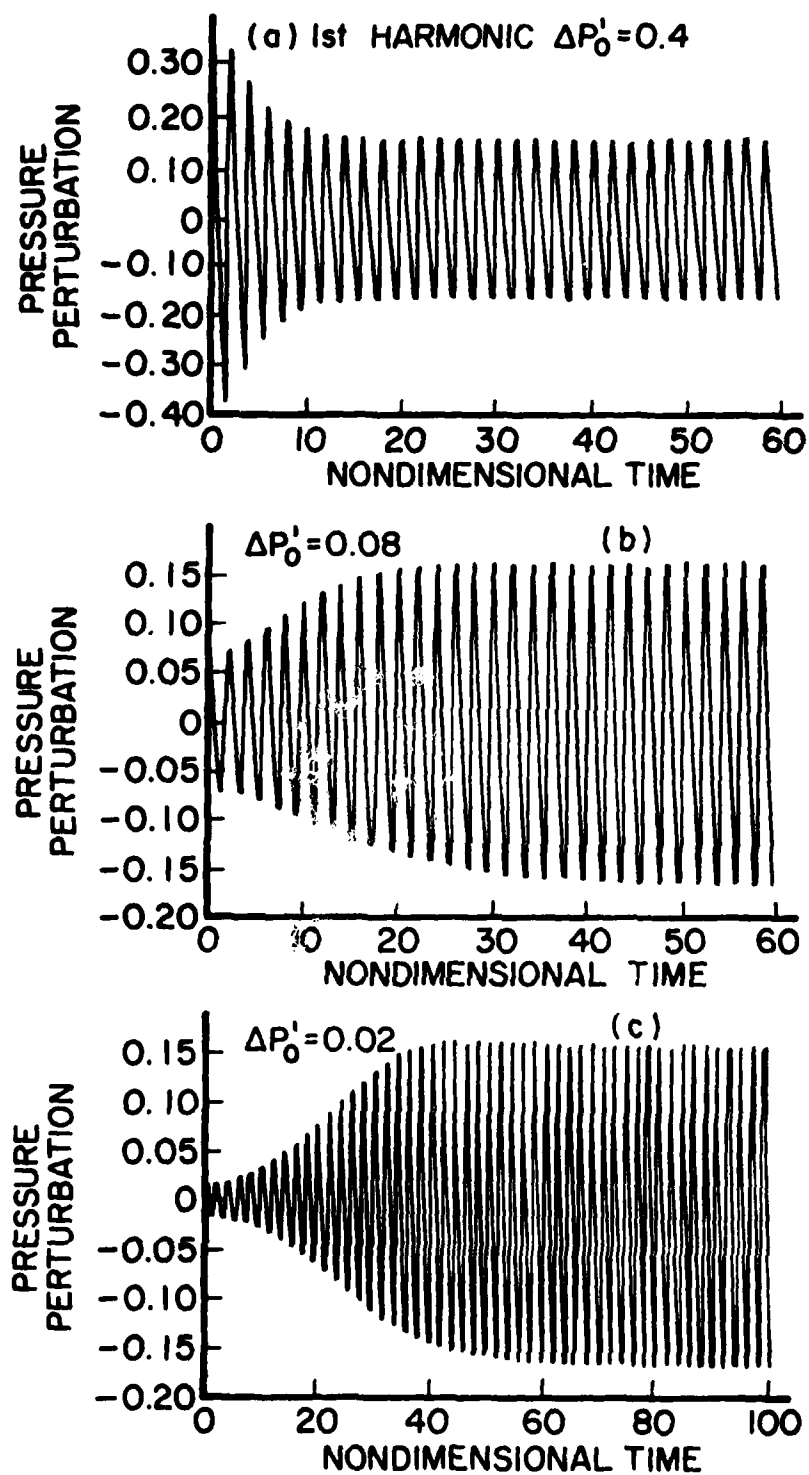
16

Figure 4. Time Evolution of Pressure Oscillations At the Head End of the Motor (No Particles).

oxide particles and 15% particle-to-gas weight flow ratio. The results shown in Figure 5 were enlightening. The computed limit cycle amplitudes were the same (30.4% of mean pressure, peak to peak) even though the initial distur bance was 40% in one case and 2% in the other. Calculations with intermediate initial disturbances also reached the same limit amplitude.

This last series of results raised serious questions concerning the validity of the conclusion reached in Reference 4. To settle the apparent conflict, the earlier results were reproduced. This time, however, the solu- tions were carried out for twice as many wave cycles, which immediately pro- vided the answer to this seeming paradox. At a nondimensional time of 70 (when the earlier solutions were terminated) the decay rate was quite small, but not zero. It was falsely assumed that continuing the solutions would not significantly alter the limit cycle amplitudes. The present calculations show that, except for initial perturbations close to 5%, the wave is either still growing or decaying at T=150. All the solutions were getting closer and closer to the same limiting amplitude, but had yet to reach it. Figure 6 shows the present results with 2-micron, 36% particle-to-gas weight flow ratio and initial disturbance amplitudes of 40% and 2% of the mean pressure. Given the previously presented results for 15% 2-micron particles, it is expected that the solutions would approach the same limiting amplitude. Furthermore, Figure 6a demonstrates that when a particular motor propellant combination is near neutral stability (i.e., very small growth or decay rate), a very long time is needed to reach a limit cycle condition.

To reinforce further the above conclusions, calculations were made for the same motor and propellant (36% of 2-micron particles) but with increased pressure-coupled response function. The increased combustion driving unbal- ances the gains and losses and, as seen in Figure 7, results in the relatively rapid establishment of a limit cycle, with an amplitude of 29.6%. Here again, limit amplitude was independent of initial disturbance amplitude.

The pressure waveforms at the limit cycle conditions for the gas-only solution (Figure 4), 15% 2-micron particle (Figure 5), and 36% 2-micron par- ticle solutions (Figure 7) were spectrally analyzed. Due to the strong fre- quency dependence of particle damping for 2-micron particles, it was expected that the limit cycle wave form with particles would contain considerably less
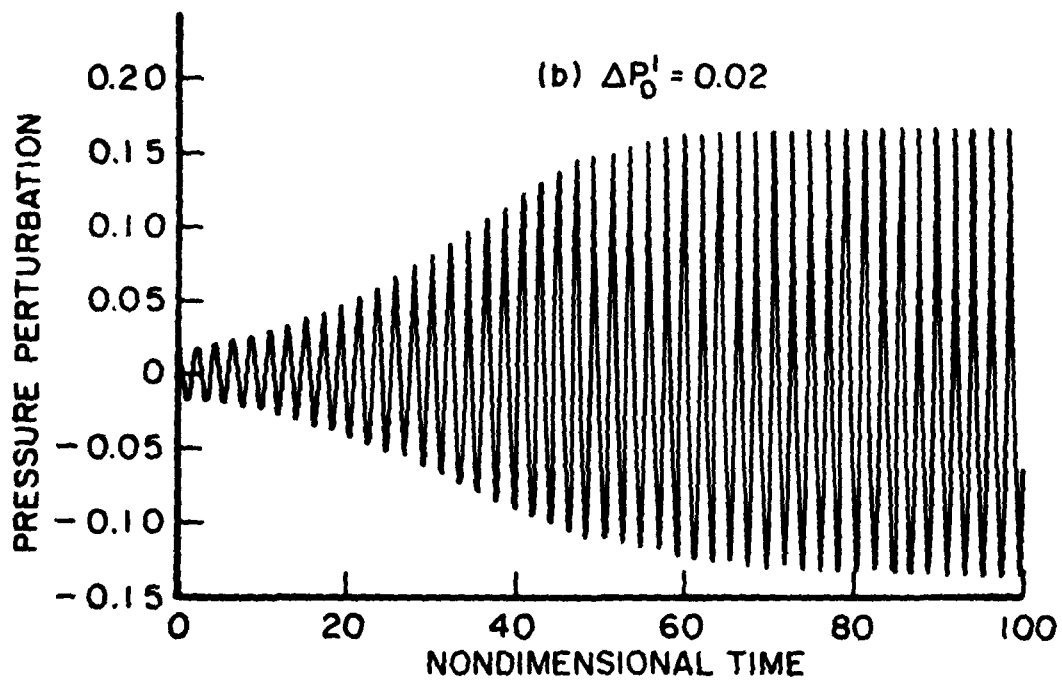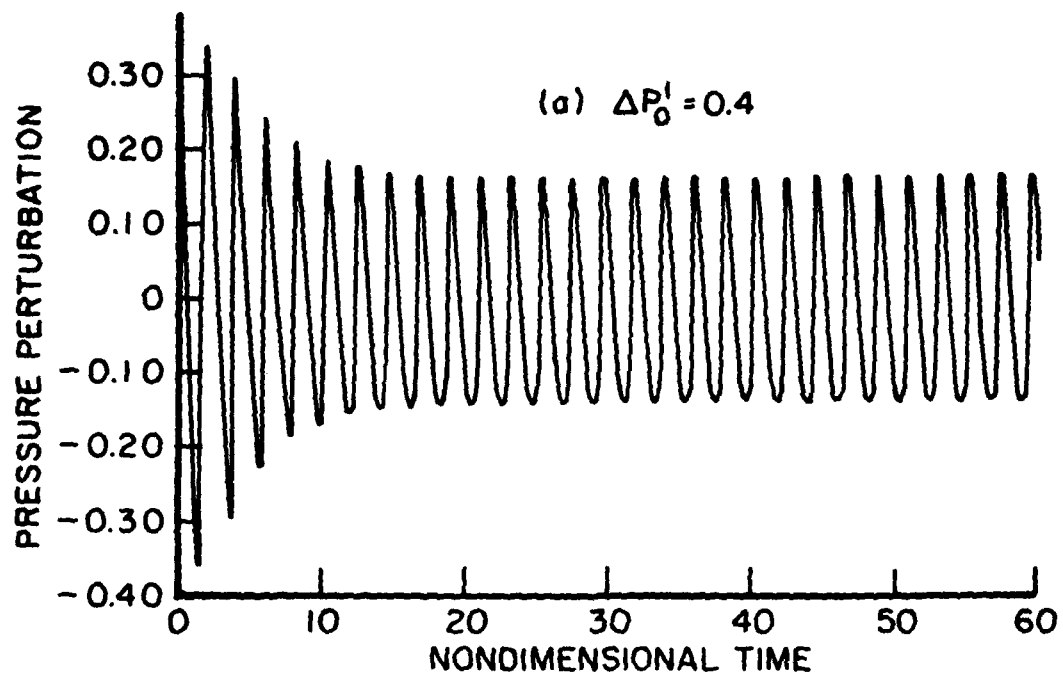
18

Figure 5. Time Evolution of Pressure Oscillations at the Head End of the Motor (15%, 2-Micron Particles).
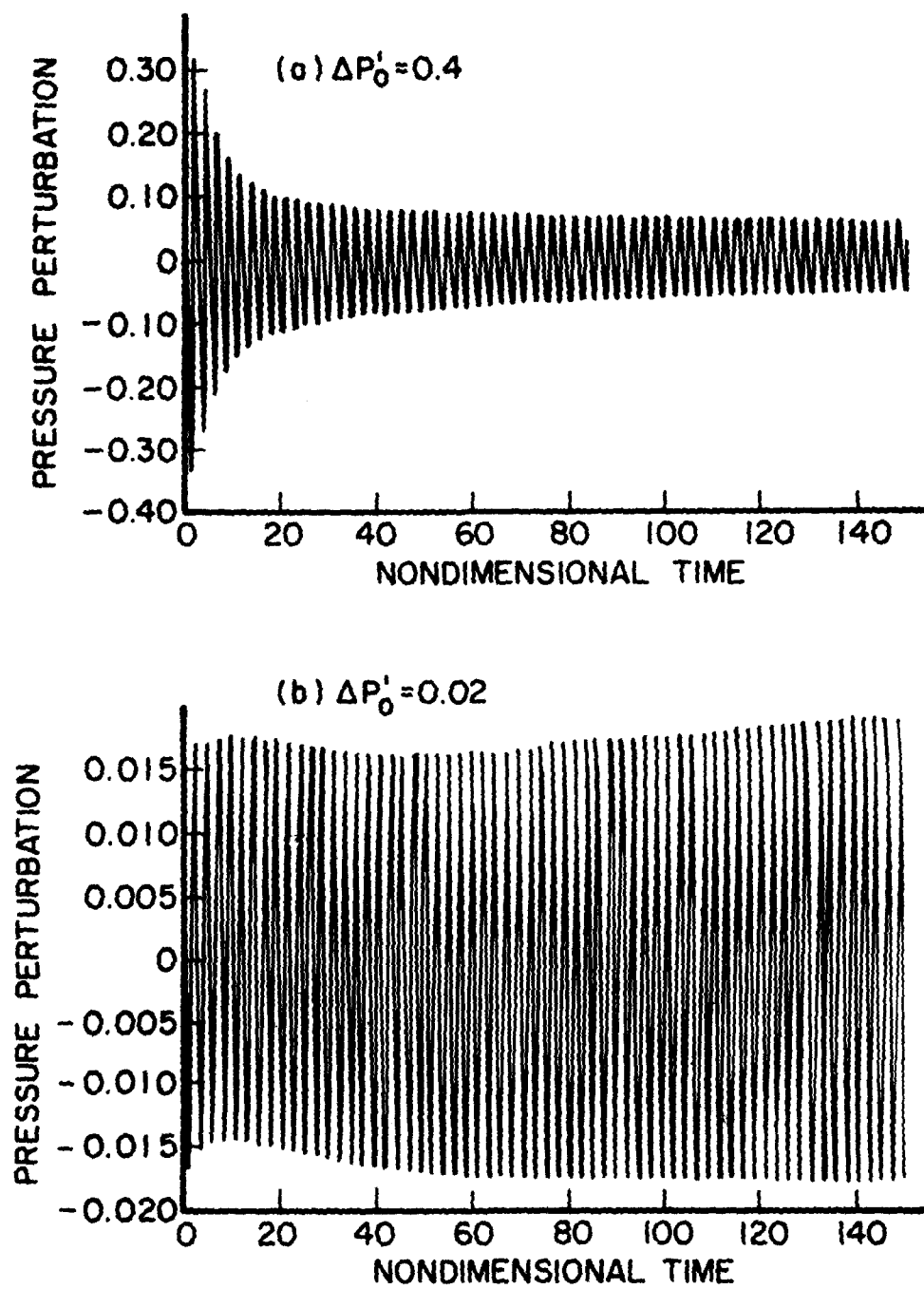
Figure 6. Time Evolution of Pressure Oscillations at the Head End of the Motor (36%, 2-Micron Particles).
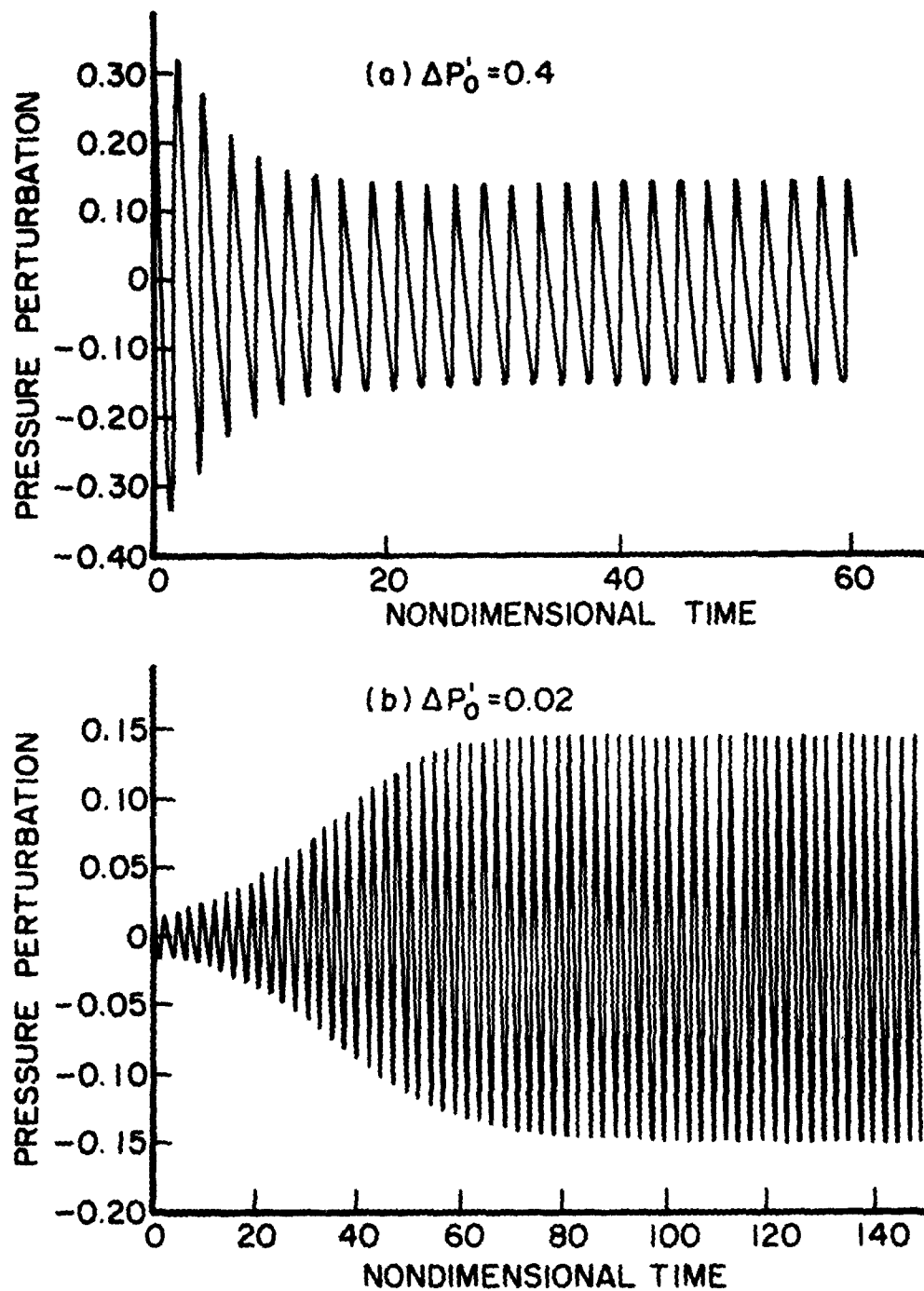
Figure 7. Time Evolution of Pressure Oscillations at the Head End of the Motor (36%, 2-Micron Particles).

21

higher harmonic content than the gas-only limiting wave form. Particle damping calculations in closed tubes[5, 24] also reinforced this expectation. Although the higher harmonic content of the solutions with particles was less than for the no-particle solution, the differences were minimal. It should be noted that to maintain the limit amplitudes at about the same level for each of these cases, the response function had to be increased with increasing particle concentration. It should also be mentioned that even without particles, the higher harmonic content of the wave forms in this motor was significantly less than that of a similar motor with larger K_n.[9] Additional calculations will be performed in the future to explore further the significance of this result.

SECTION 4
AD HOC VELOCITY-COUPLING MODELS

If velocity oscillations affect the transient burning rate of solid propellants, they must, in one way or another, enhance the heat transfer from the gas phase to the propellant. Symbolically, the energy balance at the propellant surface is written as:

$$K_g \left.\frac{\partial T}{\partial X}\right|_- \quad = \quad K_g \left.\frac{\partial T}{\partial X}\right|_+ \quad + \quad \rho_s r Q_s \qquad (1)$$

heat transfer to solid pro- pellant	heat transfer from gas phase to surface	total energy released at surface

The term $K_g \left.\frac{\partial T}{\partial X}\right|_+$ has to be modified to incorporate the effect of acoustic velocity fluctuations. In the absence of a fundamental physical model, a number of functional forms were considered for the dependence of $K_g \left.\frac{\partial T}{\partial X}\right|_+$ on u'. Since a functional form of the following type has sometimes been successful in rationalizing observed events, it was considered first.

$$\left[K_g \left.\frac{\partial T}{\partial X}\right|_+ \right]_{vc} \sim \left[\epsilon_1 \, (u-u_t) - \epsilon_2 \, (\bar{u}-u_t) \right]$$

$$\text{where} \quad \epsilon_1 = \begin{array}{l} 0, (u < u_t) \\ 1, (u > u_t) \end{array} \qquad (2)$$

$$\text{and} \quad \epsilon_2 = \begin{array}{l} 0, (\bar{u} < u_t) \\ 1, (\bar{u} > u_t) \end{array}$$

Here u is the total velocity, $u = \bar{u} + u'$; $\bar{u}$ is the mean velocity, and u' the local acoustic velocity fluctuation. The term u_t represents a threshold velocity which, in reality, may or may not exist. Justification for this functional form may be found in several references.[22, 27]

---

27. Medvedev, Yu. I. and Revyagin, L. L., "Unsteady Erosion of a Powder," Fizika Goreniya i Vzryva, Vol. 10, No. 3, pp. 341-345, May-June 1974.

When $u' \gg u$ and $u_t = 0$, Equation (2) can be approximated by:

$$K_g \frac{\partial T}{\partial X} + vc \approx u'$$ (3)

According to linear analysis, a term such as shown in Equations (2) and (3) can be added only to the heat transfer. However, in nonlinear analysis, a velocity-coupled heat transfer term could be incorporated on an additive or multiplicative basis. It was decided to insert a term on a multiplicative basis. The following functional form was adopted:

$$K_g \frac{\partial T}{\partial X} + pc+vc = \left[K_g \frac{\partial T}{\partial X} + pc \right] \left[1 + \frac{R_{vc}}{R_{pc}} \theta_{vc} F(u) \right]$$ (4)

where $F(u)$ is given by Equation (2) or (3), R_{pc} is the pressure-coupled response function, and R_{vc} is the linear velocity-coupled response function.

For small amplitude oscillations, $u' < u$ and $u_t = 0$, the right side of Equation (2) reduces to u'. Thus, using the combustion model evaluated in the linear limit,[11] it can be shown that for R_{vc} to be equal to R_{pc}, θ_{vc} in Equation (4) must satisfy

$$\theta_{vc} = \frac{2n(1-H) + \dfrac{C_p (n-n_s)}{C_s A}}{(1-H)}$$ (5)

In the small amplitude linear limit, Equation (4), combined with the present combustion model, reduces to the velocity-coupled model used by Culick,[6] and Levine and Culick.[4]

Equations (4) and (5) together with either (2) or (3) were termed the heat transfer augmentation model. For reasons to be discussed in the next section, results were also obtained with the following equation:

$$W_{pc}+vc = W_{pc} \left[1 + R_{vc} F(u) \right]$$ (6)

W is the instantaneous propellant mass burning rate ($W=W+W'$), and W_{pc} is the instantaneous mass burning rate computed from the existing pressure-coupled

24

model. With F(u) given by Equation (2) Equation (6) reduces, in the low amplitude limit, to the linear velocity-coupling model used in the past. The key difference between Equation (6) and Equation (4) is that the velocity-coupling effect built into Equation (6) directly modifies the propellant burning rate rather than affecting it indirectly through a model developed for pressure-coupled response function prediction. Equation (6) has been termed the burn rate augmentation model.

SECTION 5
VELOCITY COUPLING RESULTS

Reference 22 presents results obtained by using both the heat transfer and burn rate augmentation models. With the heat transfer augmentation model, neither triggering nor measurable mean pressure shifts could be produced, even with a velocity-coupled response function of 19.8. With the burn rate augmentation model, results exhibiting triggering and mean-pressure shifts were obtained with velocity-coupled response functions as low as 5. It was concluded that the inability of the heat transfer augmentation model to produce significant nonlinear velocity-coupling effects is symptomatic of deficiencies resulting from the use of a quasi-steady gas phase, homogeneous solid phase, combustion model. Results from further investigations reported herein provide some insight into the posible nature of the deficiencies.

The results shown in Figures 8a and 8b were obtained for a constant cross-sectional area cylindrically perforated motor, 23.5 inches (0.597 m) long. The reasons for selecting a cylindrical configuration to start with were: (a) it is the simplest possible motor configuration, (b) a large body of pressure-coupled-only solutions was available for these configurations, (c) linear velocity coupling theory[28] yields no effect of velocity coupling for such configurations. Thus, any velocity-coupling effects observed would be due to nonlinear effects, and (d) although cylindrical motors often show little evidence of velocity coupling, in many recorded instances severe triggered instabilities, with large mean pressure shifts, have been observed in such motors.[13-15, 22]

With a linear pressure-coupled response function of 3.3 and no velocity-coupling, this motor-propellant combination reached a limit amplitude of 21.73% of mean pressure, peak-to-peak. With the heat transfer augmentation model and a velocity-coupled response function equal to 3.3 (Figure 8a), the calculated wave form is almost identical to the one obtained with pressure-

28. Lovine, R. L., "Standardized Stability Prediction Method for Solid Rocket Motors," Vol. I, AFRPL-TR-76-32, May 1976.
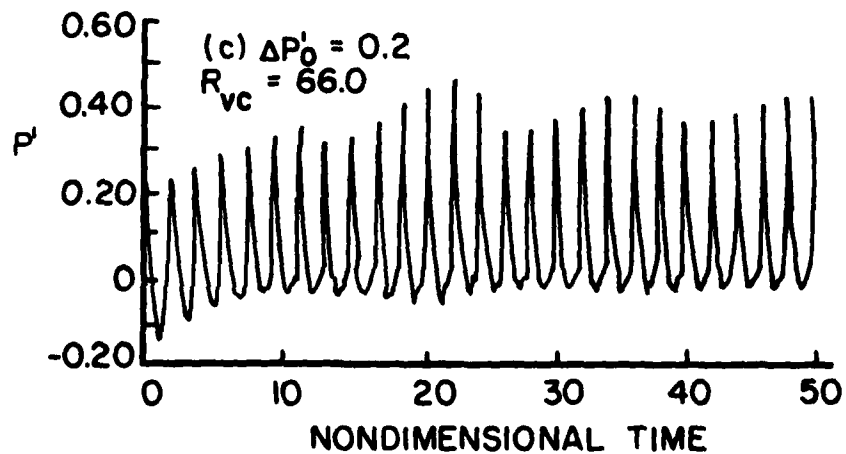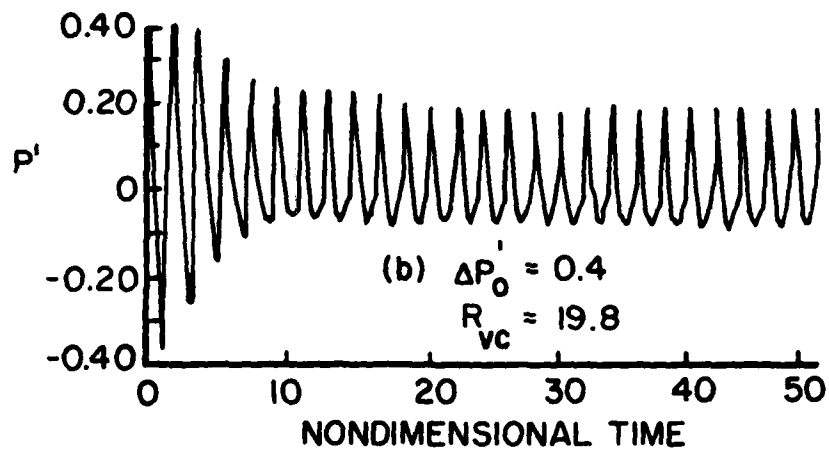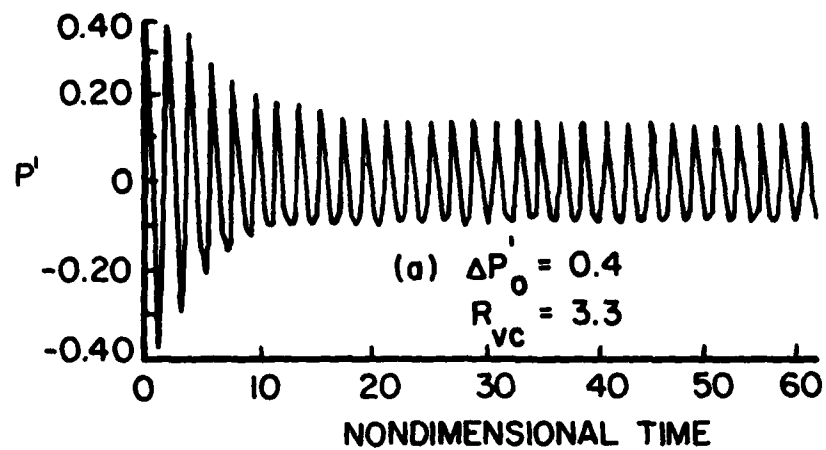
Figure 8.   Time Evolution of Pressure Oscillations at the Head End of the
            Motor.   Velocity Coupling Augmenting the Heat Transfer to the
            Propellant Surface.

coupling alone. The peak-to-peak limit amplitude was increased by only 1.2%. Raising the velocity-coupled response to 19.8 increased the change in peak-to-peak amplitude to 7.3% (Figure 8b). Nevertheless, even at this high response value, no measureable dc pressure shift was observed.

To explore further the reasons for this behavior, additional solutions have been obtained with extremely high values of R_{vc}. At a value of $R_{vc} = 40$, strong nonlinear effects and a measureable dc shift were produced. At $R_{vc} = 60$ (Figure 8c), a significant dc pressure shift is observed, as well as a modulated limit cycle amplitude. These results are similar to those obtained with the burn rate augmentation model with significantly lower velocity-coupling response function values (as low as $R_{vc} = 5$).

Based on these results, it has been concluded that the relative ineffectiveness of the heat transfer augmentation model is a result of the response function versus frequency characteristics implied by Dennison and Baum type models. With such quasi-steady combustion models, the gas phase heat transfer (whether from pressure- or velocity-coupled effects) produces a response function versus frequency curve that has a single narrow peak. Figure 9 depicts the response function versus frequency curve for the parameters used in the calculations shown in Figure 1 (A = 5.975, B = .53). At the nondimensional frequency implied by the propellant burn rate parameters and motor operating conditions used in the calculations ($\Omega = 3.78$), the pressure-coupled response function was equal to 3.3. At the second harmonic frequency, $\Omega = 7.56$, the response function is only 0.3, while at the higher harmonics, it is even lower. With the heat transfer augmentation model, the velocity-coupled response function is, to first order, proportional to the pressure-coupled response. (Note: for the problems being considered, the waves are primarily traveling rather than standing, and the velocity is approximately in phase with the pressure over half the cycle and 180° out of phase with the pressure over the other half of the cycle.) Thus, for the problem that was solved, the velocity-coupled response for the second harmonic was about a factor of 10 lower than the response function at the fundamental frequency.

With the mass transfer augmentation model, Equation (6), the velocity-coupling response is independent of the combustion model, and to first order is independent of frequency. Thus when a velocity-coupled response function

28

of 5 was specified, this was the approximate value at all frequencies. Given the nature of Figure 9, it would require a value of $R_{vc}/R_{pc} = 16.6$ (which implies $R_{vc} = 55$ for the first harmonic) for the heat transfer augmentation model to produce a similar value of $R_{vc} = 5$ for the second harmonic.

The above discussion appears to explain the wide disparity between the results obtained with the two ad hoc models. Furthermore, it implies that a realistic velocity-coupling model will have to be capable of providing strong driving at the higher harmonic frequencies.

The results presented in this report were obtained with a constant cross-sectional area grain for which linear velocity coupling is zero with the ad hoc models for both standing and traveling waves. Thus, the observed results are attributable to nonlinear velocity-coupling effects. In variable area grains, linear as well as nonlinear velocity-coupling effects may be observed. Nevertheless, it is expected that even in such cases, significant nonlinear velocity-coupled response will require strong driving at the higher harmonic frequencies. This hypothesis will be explored in the near future.

To further our understanding of the velocity-coupling problem and nonlinear instability in general, the previously obtained solutions[22] were examined in detail, not only at the head and aft ends, but also at the one quarter, one half, and three quarter points. Figures 10, 11a, and 11b represent an interesting series of results. These solutions are for the same motor and propellant combination as the Figure 1 calculations, but with a pressure-coupled response function of 2.18. With this pressure-coupled response and no velocity-coupling, the motor is stable, even at an initial disturbance amplitude as high as 40% of the mean pressure (Figure 10). Figures 11a and 11b were obtained using the burn rate augmentation model for velocity-coupling with $R_{vc} = 5$ and $F(u)$ given by Equation (3). With an initial disturbance amplitude of 2% (note that all of the initial disturbances were first harmonic standing waves), the wave grows slightly initially, but then damps (Figure 11a). Overall, the result is a stable motor. With an initial disturbance amplitude of 5% (Figure 11b), the oscillations rapidly grow, appear to reach a limit amplitude, but then grow again. In addition, a mean pressure shift of about 12% is observed. These results demonstrate triggering at a finite initial disturbance amplitude, steep-fronted waves, mean pressure shift
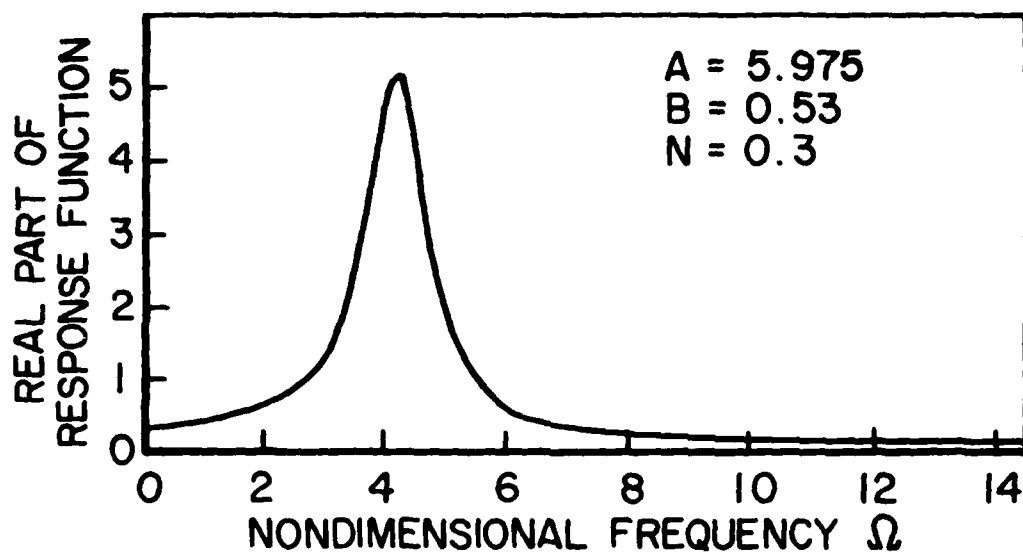
29

Figure 9. Typical Response Function Versus Frequency Curve for a Solid
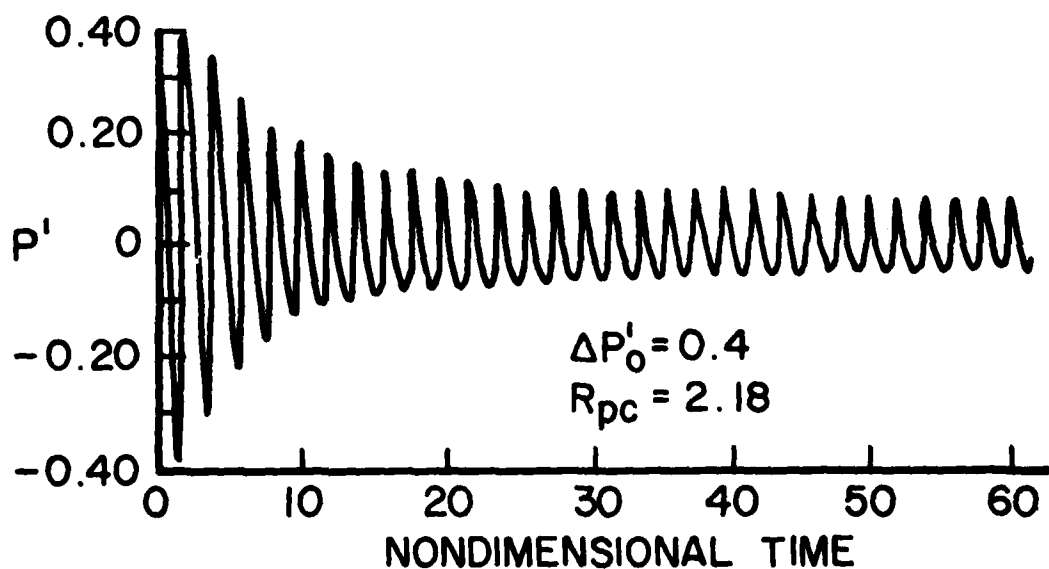Propellant as Calculated Using Dennison and Baum Type Models.

Figure 10. Time Evolution of Pressure Osciilations at the Head End of the
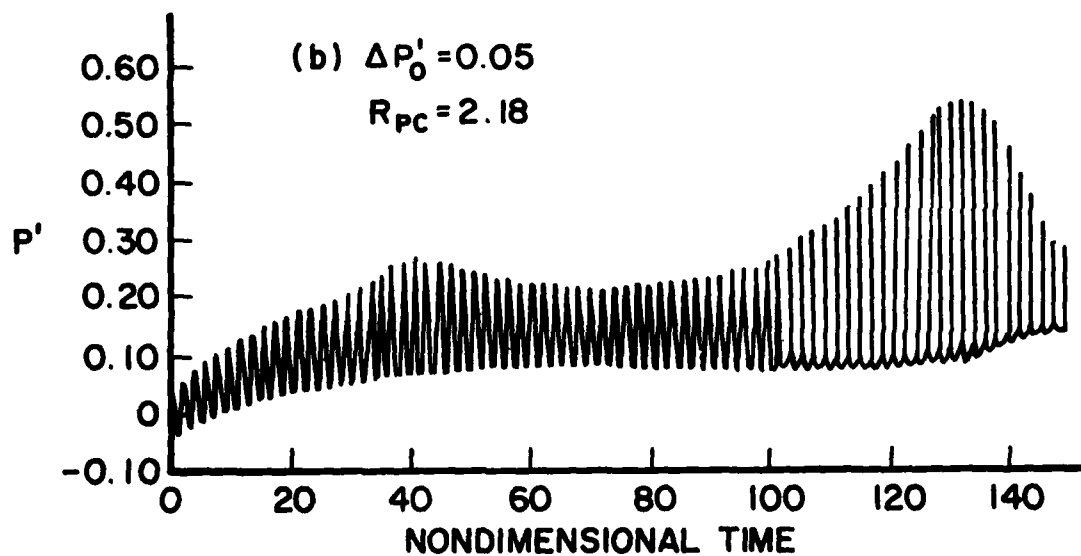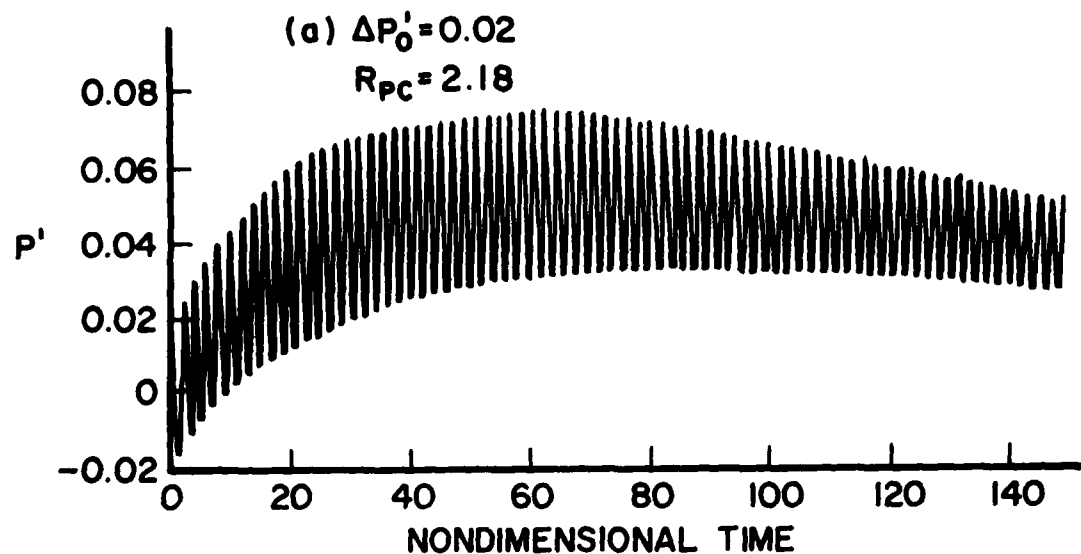Motor, Pressure Coupling Only.

Figure 11. Time Evolution of Pressure Oscillations at the Head End of the Motor. Velocity Coupling Augmenting the Transient Burn Rate. $F(u) = |u'|$, $R_{VC} = 5.0$.

and a lack of a steady limit cycle, all characteristics often observed in motor data.

The behavior demonstrated in Figures 11a and 11b is very complex and is, undoubtedly, the result of many mutually interacting nonlinear fluidynamics and combustion phenomena. Some of the complexity of the problem is illustrated in Figures 12 and 13, which present expanded views of the pressure, burning rate, and velocity (actually $F(u) = |u'|$) wave forms at the head end, 1/4, 1/2, and 3/4 points and aft end, for the cases previously presented in Figures 11a and 11b. The wave forms are shown in the interval around a nondimensional time of 30 (15 wave cycles).

If the oscillations were standing waves, the velocity oscillations would be 90° out of phase with the pressure. On the other hand, if the oscillations were being produced by a traveling wave, the pressure and velocity would be in phase for half of a wave cycle, and 180° out of phase for the other half of the cycle (Figures 12 and 13 show $|u'|$ rather than u'; thus $|u'|$ should be in phase with p' for the whole cycle). The phase relationship between p' and m' is a very complex function of the frequency, amplitude, and phase of the pressure and velocity waves and the characteristics of the propellant. From a stability standpoint, the phase relationship between p' and m' is critical, since the combustion driving is produced by the component of m' that is in phase with p'. The figures were designed only to display the phase relationships between the oscillations; the amplitude scales for each curve are different and are not indicated.

From Figure 12 (stable) and Figure 13 (unstable), it can be seen that the waves are primarily, but not completely, traveling waves, since the velocity is close to being in phase with the pressure. This is true even though the calculations were initiated with a standing wave disturbance, and for the stable case, even though the waves are not steep fronted and are of relatively low amplitude. In addition to the differences in wave forms, there are some other significant differences between the two sets of results. At the head and aft ends, where the velocity oscillations are zero or very small, respectively, the phase relationship between m' and p' is still quite different for the two cases. In the stable case (Figures 12a and c), the burn rate leads the pressure by about 51°, while in the unstable case (Figures 13a
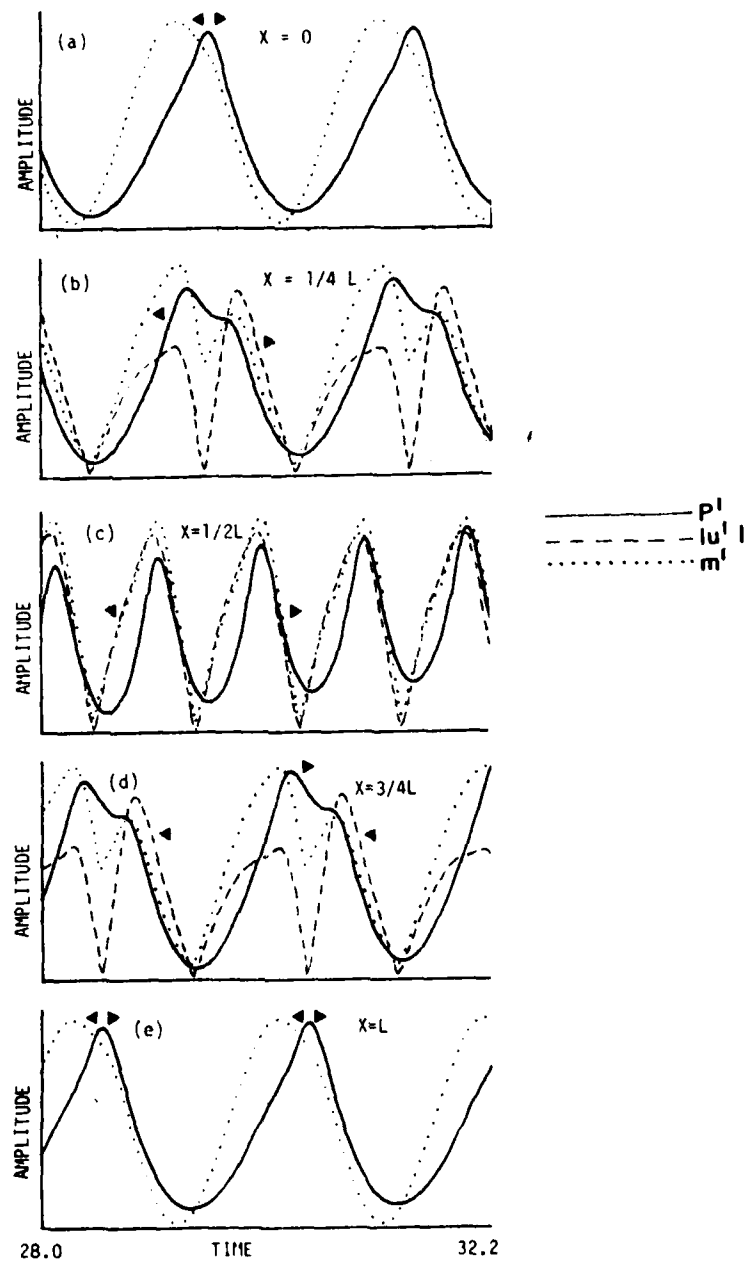
32

Figure 12. Expanded View of the Pressure, Burning Rate, and Velocity ('u')
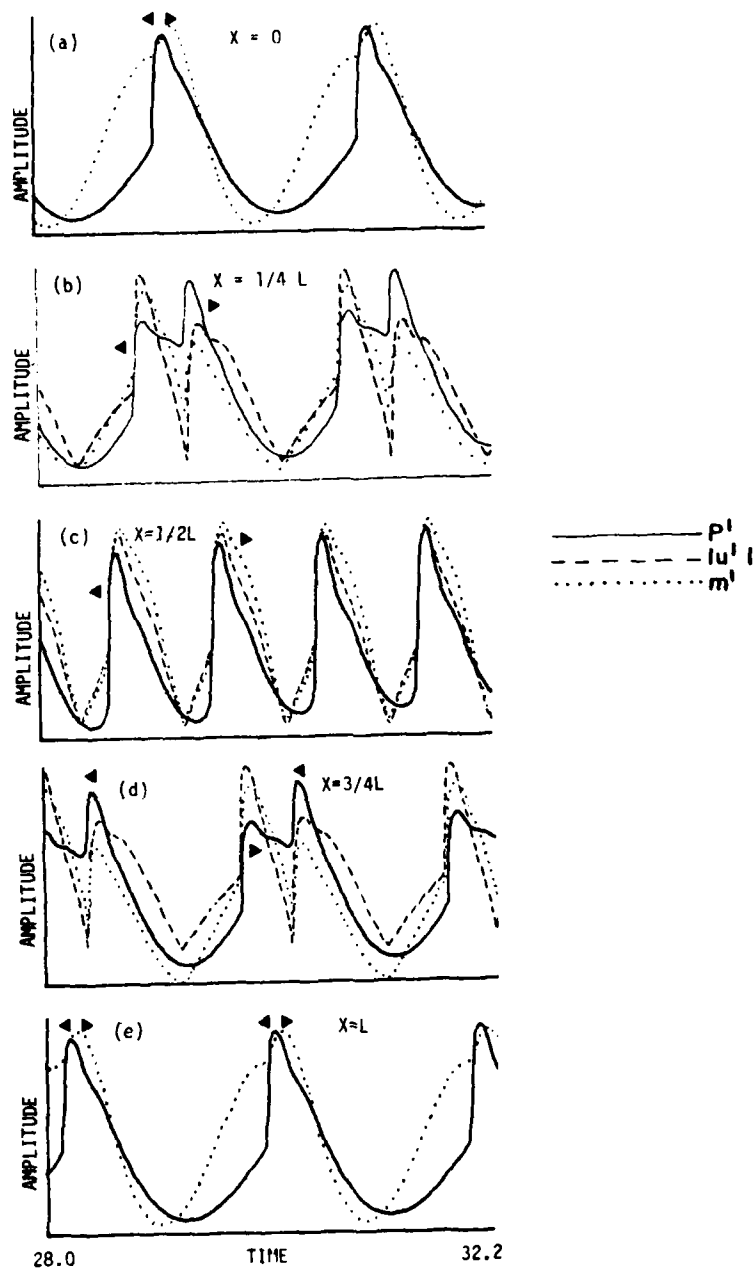Waveforms After 15 Wave Cycles, for a Stable Solution (Fig. 4a).

Figure 13. Expanded View of the Pressure, Burning Rate, and Velocity (ιu'ι)
Waveforms After 15 Wave Cycles, for an Unstable Solution
(Fig. 4b).

34

and c), the burn rate lags the pressure, but only by 8`. At these points
(X = 0, X = L) the difference in phase between the two cases can only be
attributed to the difference in the pressure wave form. At the 1/4 point, the
results are somewhat more complicated. For the unstable case (Figure 13b),
the amplitude of the pressure wave is lower when it is traveling towards the
head end than after it has been reflected off the head end and is traveling
back towards the nozzle. The behavior of the burning rate and velocity wave
forms for this case is just the opposite, i. e., they are lower after reflec-
tion than before it. For the stable case (Figure 12b), both the pressure and
burning rate are lower after reflection, while the velocity is higher after
reflection than before it. In addition to the differences in the behavior of
the wave amplitudes, the phase relationships in the two cases are also
different. In the unstable case (Figure 13b), the burning rate is almost
exactly in phase with pressure over the whole wave cycle, while in the stable
case (Figure 12b), the burning rate leads the pressure by about 20` when the
wave is traveling towards the head end and lags the pressure by about 20` when
the wave is traveling towards the nozzle. In the unstable case, the velocity
leads the pressure by about 10` when the wave is traveling to the left, and
lags the pressure by about 10` when it is traveling to the right. In the
stable case, the velocity lead/lag is the same with regard to the
direction of travel, but the magnitude of the lead or lag is about double
(about 20`).

At the center of the motor (Figures 12c and 13c), the wave amplitudes are
almost the same, regardless of the direction of travel, and the phase dif-
ferences essentially disappear. In the center, the pressure, velocity, and
burning rate are all in phase, in both cases. At the 3/4 point, the amplitude
and phase behavior for the two cases are similar to those at the 1/4 point,
but in an antisymmetric fashion in regard to direction of wave travel.

Just from examining these two cases at one point, it becomes apparent how
complex nonlinear wave propagation can become. The waves are, in general,
some combination of traveling and standing waves. The frequency content of
the waves and the phase relationships of the pressure, velocity, and burning
rate vary significantly from one point in the motor to another, and for the
same motor, vary as a function of the initial disturbance amplitude. In

35

addition, the phase angle between m', u', and p' varies intracycle, i. e., from one portion of the wave cycle to another, and also varies in time from one cycle to another. This nonstationary behavior of the phase angle is the most likely cause of the modulated limit cycle amplitudes observed in the nonlinear velocity-coupling solutions. Results such as those presented above help to demonstrate clearly why attempts to solve nonlinear instability problems using techniques and understanding based on linear analyses cannot be expected to be uniformly successful.

SECTION 6
THRESHOLD EFFECTS

The previous velocity-coupling discussion, and the discussion in Reference 22, were for zero threshold velocity. Since threshold effects have been observed,[27] a brief attempt was made to examine their effect within the context of the present ad hoc models. The results presented in Figures 14 and 15 were obtained for the motor used in the other cases presented. The burn rate augmentation model was used with $F(u)= |u'| -u_t$. With the same pressure and velocity coupling values used in obtaining the results presented in Figure 11 (R_{pc} = 2.18, R_{vc} = 5), an unstable result could not be achieved with a threshold velocity equal to 0.02 (u_t is normalized by the steady-state gas sound speed, so u_t = .02 corresponds to about 60 ft/sec). R_{vc} was then increased to 13 and the calculations repeated in this case, with u_t = .02 and $\Delta P = 0.02 \bar{P}$; a stable result was again achieved (Figure 14a). However, when ΔP was increased to 0.08, a highly nonlinear instability was produced (Figure 14b). The threshold velocity was then increased to 0.05. With the increased threshold velocity an unstable result could not be achieved, even with initial perturbations as large as 40% (Figure 15).

Although threshold effects, if they exist, are not expected to be a function of only mean and/or fluctuating velocity, these results indicate that, as expected, threshold effects act to increase the magnitude of the velocity-coupled response function required to trigger an instability. The results also imply that propellants with high thresholds will be difficult or impossible to trigger. Threshold effects, variations in R_{vc} as a function of frequency, and nonlinear fluid dynamic effects, all interact to determine the nonlinear stability of a given motor propellant combination.
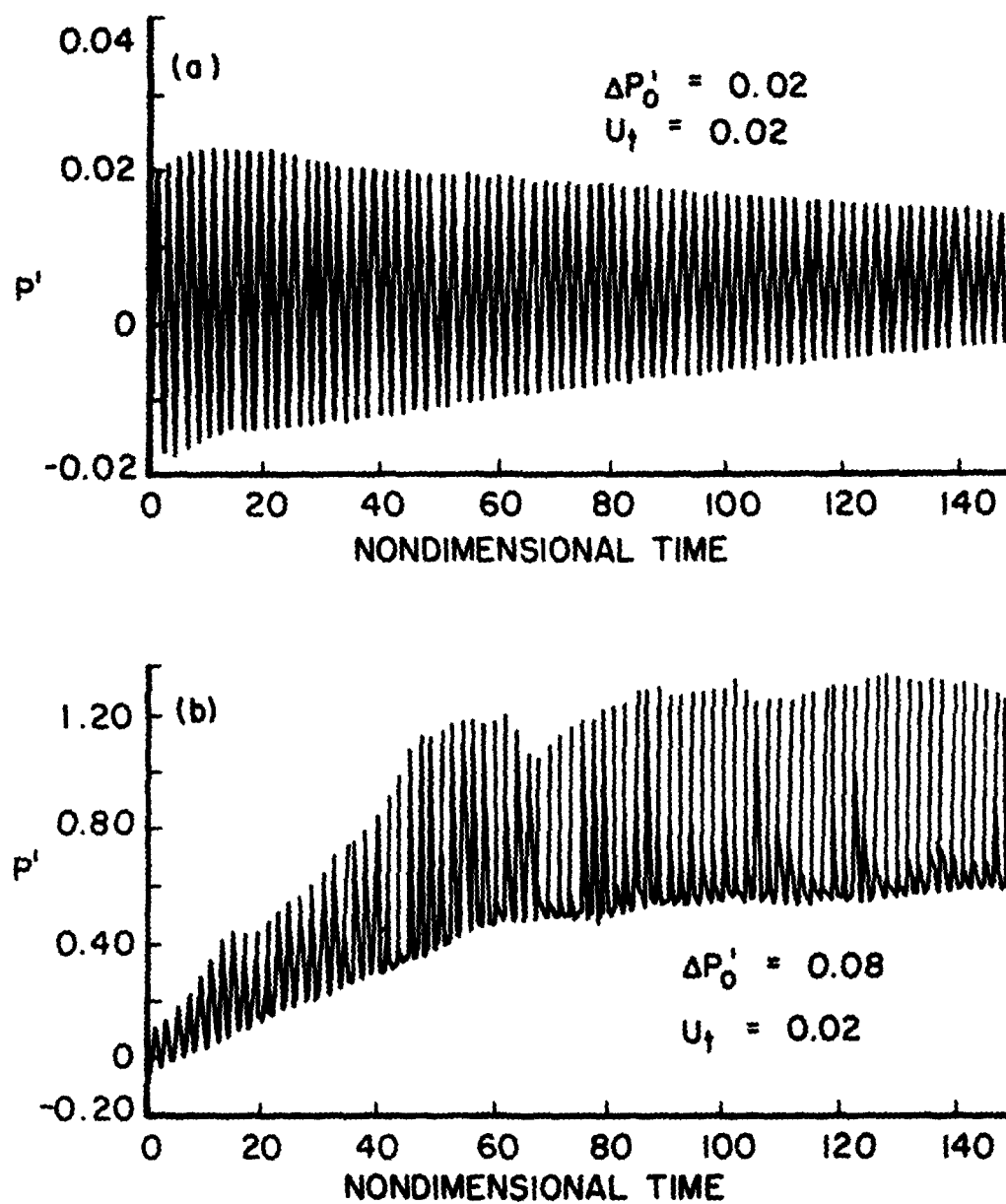
Figure 14. Time Evolution of Pressure Oscillations at the Head End of the Motor. Burn Rate Augmentation Model with Threshold Velocity, $R_{vc} = 13$.
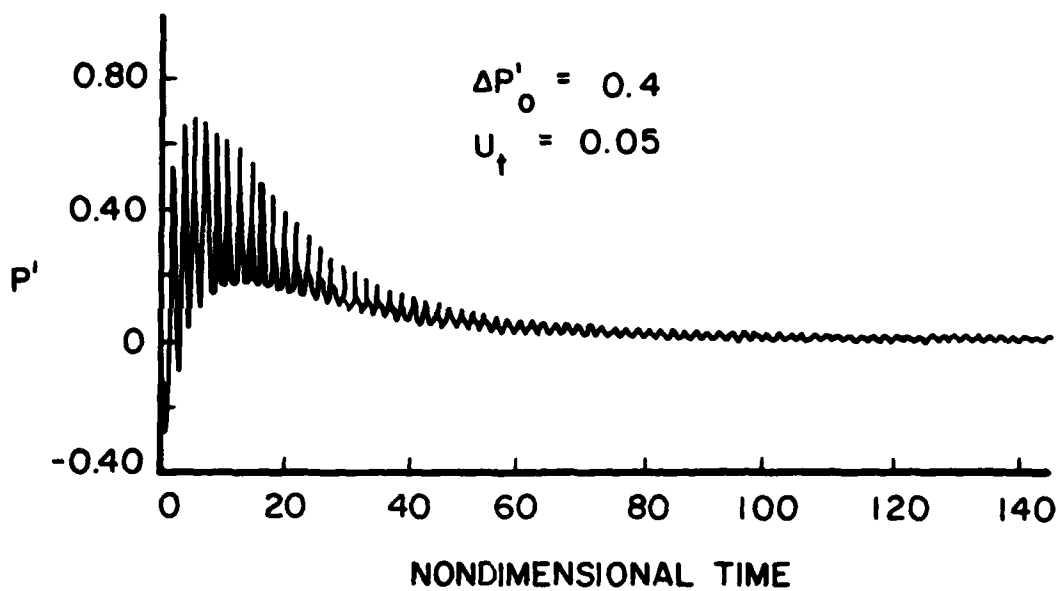
38

Figure 15. Time Evolution of Pressure Oscillations at the Head End of the Motor. Burn Rate Augmentation Model with Threshold Velocity, $R_{vc} = 13$.

SECTION 7
CONCLUSIONS

The complexity of nonlinear instability in solid propellant rocket motors and the large number of mutually interacting physical phenomena which control it make it very difficult to form generally valid quantitative conclusions, even from a relatively large number of numerical or experimental results.

The following conclusions can, however, be drawn from the large number of nonlinear instability solutions obtained during the present investigation.

1. The Lax-Wendroff + Hybrid + Artificial Compression finite difference technique can accurately predict the propagation of multiple shock waves in variable cross-sectional area rocket motor chambers.

2. The present nonlinear stability analysis is able to predict the tendency of motors with area discontinuities to form multiple shock waves. The solutions also demonstrate the complex axial variations in pressure oscillation spectra that can be expected in variable area motors.

3. Based on many more solutions than had been available in the past, it is concluded that pressure oscillations will reach a limiting amplitude independent of the characterstics of the initiating disturbance. This conclusion appears to hold for unmetallized as well as metallized solid propellants, but cannot as yet be generalized to include cases in which strong nonlinear velocity coupling is present (see number 7 below).

4. Velocity-coupling models based on quasi-steady gas phase, homogeneous solid phase, assumptions are not capable of producing strong nonlinear effects at realistic values of velocity-coupled response function.

5. A realistic velocity-coupling model must be capable of predicting high combustion response over a wide frequency range for propellants known to be able to produce strong nonlinear velocity-coupling effects.

6. Nonlinear oscillations in solid rocket motors are very complex. The oscillations are, in general, a combination of traveling and standing waves, with the traveling component being dominant, even for non-steep-fronted waves at relatively low amplitude.

7. The phase angles between the pressure and velocity and burning rate oscillations vary from one location in the motor to another, and are nonstationary in time. The nonstationary behavior of the phase angles is the most likely cause of the modulated limit cycle amplitudes observed in the solutions and in motors.

8. Solutions obtained using a threshold velocity imply that propellants with a high threshold will be difficult or impossible to trigger unless they also have a very high level velocity-coupled response.

(Conclusions 4 through 8, regarding velocity-coupling, are based on the results with ad hoc models and constant cross-section motors.)

DATE FILMED

7-8